The Journal of Agricultural Science

www.cambridge.org/ags

Yield decline in short wheat rotations: the impact of source and sink limitation

Katharina Pronkow[1], Josephine Bukowiecki[1], Nora Honsdorf[2] and Henning Kage[1]

[1]Institute of Crop Science and Plant Breeding, Agronomy and Crop Science Group, Kiel University, Kiel, Germany and [2]Institute of Organic Farming, Johann Heinrich von Thuenen Institute, Westerau, Germany

Crops and Soils Research Paper

Cite this article: Pronkow K, Bukowiecki J, Honsdorf N, and Kage H (2025). Yield decline in short wheat rotations: the impact of source and sink limitation. *The Journal of Agricultural Science* **163**, 381–392. https://doi.org/10.1017/S0021859625100142

Received: 15 January 2025
Revised: 21 May 2025
Accepted: 4 June 2025
First published online: 11 July 2025

Keywords:
crop rotation; food security; Monteith equation; radiation interception; yield formation

Corresponding author:
Katharina Pronkow;
Email: pronkow@pflanzenbau.uni-kiel.de

Abstract

A growing demand for wheat as a staple crop leads to an expansion of its production. The consequence is land use change and short rotations for wheat. But wheat grown in short rotations causes yield decline. To secure future food supplies, a deeper understanding of the physiological processes contributing to this yield reduction is needed. Therefore, a three-year data set from a long-term field trial in Northern Germany was analysed to investigate the impact of crop rotational position (CRP) (wheat grown in the first [W1] and in the third [W3] year in self sequence after break crop) in combination with three genotypes and four rates of nitrogen (N) fertilizer on intercepted radiation by the canopy (Q), radiation use efficiency (RUE), grain yield and yield components. All genotypes showed a reduction of Q, RUE and yields in W3. The focus was further set on differences in yield formation pre- and post-anthesis. This revealed a significant interaction between CRP and genotype. An overall reduction in intercepted radiation pre-anthesis as well as in kernels/m^2 in W3 suggested, that yield formation under adverse pre-crop conditions was rather ‘source limited’. A possibility to compensate this limitation might be a prolonged phase of radiation interception post-anthesis.

Introduction

Wheat (*Triticum aestivum*) as one of the most important staple crops worldwide showed a linear yield increase during the second half of the last century (Calderini and Slafer 1998). This has helped to secure the demand of a growing population, keeping food prices low and reducing land use change (Fischer 2020). Since the late 1990s, this yield progress stagnated in high-yielding environments (Brisson *et al.* 2010; Calderini and Slafer 1998) even though breeding progress is still linear (Rose and Kage 2019; Voss-Fels *et al.* 2019). As possible causes, climate change (Bönecke *et al.* 2020), changes in agricultural policy (Moore and Lobell 2015) or wheat grown in shorter rotations (Fischer *et al.* 2014) have been discussed.

Fischer 2020 mentioned increasing yields of wheat for the latest period between 2002 and 2016 compared to the stagnation in the years between 1986 and 2001. Potential factors explored by the author were the expansion of the production area and significant increases in global grain prices in 2008 and 2010. Given the current high prices and continuing demand for wheat, it appears probable that wheat production will continue to expand in the foreseeable future. This expansion can only be achieved at the cost of converting more land into cropping area or adopting shorter crop rotations.

Wheat grown after wheat is known to decline in yield. The extent depends on site, weather conditions and crop management (Bennett *et al.* 2012; Christen 1998; Sieling *et al.* 2005). Therefore, wheat grown after break crops shows up to 20 % higher yields compared to wheat after cereals with a smaller benefit in semi-arid areas or dry seasons (Kirkegaard *et al.* 2008). In contrast, Sieling *et al.* 2005 reported higher yield losses for wheat grown after wheat in drier years with a negative water balance (rainfall minus transpiration from May to July) compared to wheat after a break crop. Several reasons for the yield benefit of break crops have been discussed. Break crops may increase nutrient pools, mainly nitrogen (N) (Bullock 1992). However, Kirkegaard *et al.* 1994 did not observe any effect of soil N differences between cereal and non-cereal pre-crops on wheat biomass at the start of stem elongation. Break crops may interrupt the life cycle of pathogens and thereby contributing substantially to disease control (Bullock 1992), but the direct link between a higher disease pressure and the observed yield decline is not easy to prove (Bennett *et al.* 2012; Bullock 1992).

A pathogen which is mainly related to yield decline in wheat grown in short rotations is the soil-borne fungus *Gaeumannomyces tritici* (*Ggt*) (Cook 2003). Currently there are no wheat cultivars for farmers available that are resistant to *Ggt* (Palma-Guerrero *et al.* 2021). As infected roots are limited in their functions, the plants are limited in N (Gutteridge *et al.* 2003) and water uptake and are more susceptible to drought (Sieling *et al.* 2005). The highest decline of grain yield in wheat grown in a monoculture, defined as the same crop grown on the same field for several years, is usually observed in the third to fourth year. The yield decline in wheat with *Ggt* infections can be caused by a reduction in ears/m^2 (Sieling *et al.* 2005; Sieling *et al.* 2007), kernel number (Christen *et al.* 1992; Sieling *et al.* 2007; van Toor *et al.* 2016) or grain weight (Christen *et al.* 1992; Kirkegaard *et al.* 1994; Sieling *et al.* 2005; Sieling *et al.* 2007; van Toor *et al.* 2016). A restriction in biomass can be observed early in the season (Arnhold *et al.* 2023b), which can be explained by the plant allocating its energy towards the expression of resistance-related genes (Gholizadeh Vazvani *et al.* 2025). In some years, a yield decline in wheat grown after wheat can even be observed without any visible symptoms of *Ggt* infections on the roots (Arnhold *et al.* 2023a).

Grain yield is formally the product of kernels/m^2 and grain weight (Fischer 2011). Analysing yield formation with this approach is often based on the hypothesis of sink limitation. Another approach is to dissect yield formation into three factors using Eq.(1):

$$Y = Q \times RUE \times HI \qquad (1)$$

where Q is the intercepted photosynthetic active radiation (PAR) by the canopy, RUE is the radiation use efficiency and HI is the harvest index (Monteith 1977). The amount of Q during the growing season depends on irradiation, the canopy size, its development until closure and how long the photosynthetic active ('green') plant material can be maintained (Long *et al.* 2006). RUE is the ability of the plant to convert the energy from the captured radiation into biomass (Arkebauer *et al.* 1994; Long *et al.* 2006) and the HI is a function of assimilate allocation and translocation during the growth period (Lo Valvo *et al.* 2018; Rivera-Amado *et al.* 2019).

This approach expresses more explicitly the hypothesis of source limitation of grain yield, as the product of absorbed PAR and RUE is a proxy of 'source' strength, but at least the HI may be influenced by the sink strength.

According to Eq.(1), the generated biomass is linearly correlated to the amount of intercepted radiation in unstressed conditions (Monteith 1977; Wilson and Jamieson 1985). Yield formation may be determined by the size of the photosynthetic active plant, referred to as 'source', the number and size of the reproductive organs and therefore the capacity to store assimilates is the 'sink' (Asseng *et al.* 2017; Reynolds *et al.* 2022; Schnyder 1993). The importance of 'source' or 'sink' for the limitation of the final yield may vary with the developmental stage of the plant (Reynolds *et al.* 2022). During stem elongation and the period pre-anthesis, the formation of grains and spikes is set and yield formation is source limited at this time. The number of grains and spikes, which have been built pre-anthesis, define the sink strength post-anthesis, which then limits the yield formation during grain-filling (Reynolds *et al.* 2022). The most sensitive phase for yield formation was first defined by Fischer 1985 as the 30 days before anthesis. Slafer *et al.* 2021 named the three weeks before until seven days after anthesis as the only period in which yield formation in wheat is source limited. Sabir *et al.* 2023 also found evidence of source limitation in yield formation several days after anthesis. After anthesis, the remobilization of stored proteins begins to fulfil the demand of the developing grain, which contributes to the final grain weight (Foulkes *et al.* 2009). In addition, Sabir *et al.* 2023 reported an impact of source strength post-anthesis on the final number of grains per area. The process of photosynthesis is restricted when the plant is exposed to environmental stress factors (Ashraf and Harris 2013; Jamieson *et al.* 1995; O'Connell *et al.* 2004; Schierenbeck *et al.* 2016; Sharma *et al.* 2020).

The aim of this study is (1) to evaluate the impact of an unfavourable crop rotational position (CRP) on components of Eq. (1) and (2) to investigate possible effects of genotypic growth patterns which can contribute to overcome CRP-related limitations.

Material and methods

Site description

Data were collected in three consecutive growing seasons (2019/20 – 2021/22) in a long-term field experiment, which was established in autumn 1989 (for further information, see Sieling *et al.* 2005). The experiment was conducted at Kiel University´s experimental station Hohenschulen (54 °18´ N, 9 °58´ E, 33 m a.s.l.) in North Germany. The site is characterized by a small-scaled heterogeneous soil. The main type is a pseudogleyic sandy loam (Luvisol: 170 g/kg clay, pH 6.8, 13 g/kg C_{org}, 1.1 g/kg N_{org} in 0 – 30 cm). The climate is humid temperate with a mean long-term annual temperature (from 1991 to 2021) of 9.4 °C and an annual precipitation of 755 mm. In all three growing seasons, the annual mean temperature was above the long-term average (+ 1 °C in 2019/20, + 0.3 °C in 2020/21, + 1.5 °C in 2021/22) whereas the annual rainfall was below the average in 2019/20 (−9.3 mm) and 2021/22 (−27.4 mm) and above the average in 2020/21 (+ 13.7 mm) (Fig. 1).

Experimental design

The crop rotation of the experiment was faba bean – oat – oilseed rape (OSR) – winter wheat (WW) – WW – WW. For this study, the data samplings were focused on the first (W1) and third (W3) years of wheat following OSR. Each of the crops were grown separately on a main plot. On each of the six main plots, the crop rotated every year according to the crop rotation. Each CRP was present in every year of the experiment. Within W1 and W3, the combination of three genotypes ('Elixer', 'Nordkap', 'Tobak') and four rates of N fertilizer (calcium ammonium nitrate (27 % N)) (Table 1) were established in subplots. Each genotype x N rate combination was randomly distributed within four replicates in the main plots. Sub plot size was 12 m × 3 m, where 9 m × 3 m were used for harvest by combine. The main plots on which OSR, the second WW after OSR, faba beans and oats were grown had a uniform management to allow for homogenous starting conditions for W1 and W3. The N fertilization of the pre-crops from W1 and W3 were executed according to local farm management practice (OSR: 2019/20: 160 kg N/ha; 2020/21: 170 kg N/ha; 2021/22: 170 kg N/ha; W2: 2019/20: 190 kg N/ha; 2020/21: 240 kg N/ha; 2021/22: 220 kg N/ha). Except for the different N fertilizer applications in W1 and W3, all other crop managements (e.g. application of herbicides, fungicides, insecticides and plant regulators, and the fertilization of the other crops) were conducted according to site-specific recommendations. Sowing dates for W1 and W3 were 24 October 2019 with 350 kernels/m^2, 01 October 2020 with 320 kernels/m^2 and 08 October 2021 with 320 kernels/m^2. Harvest dates were 08 August 2020, 13 August 2021 and 10 August 2022. After harvest, all residues of all crops remained on the plots.

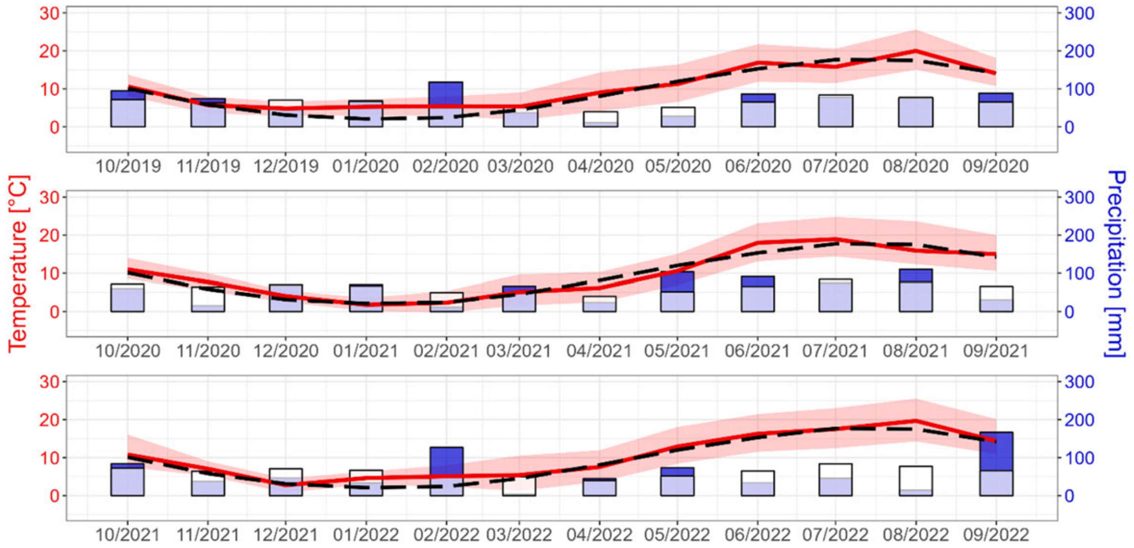

Figure 1. Monthly air temperature (red line: mean, red ribbon: max and min) and monthly precipitation sum (blue bars) of the three growing seasons (October - September) compared to the long-term average (1991 – 2021) temperature (dashed black line) and precipitation sum (white bars).

Data collection

Site conditions

The experimental farm 'Hohenschulen' is situated in a young moraine landscape with small-scale variability of soil type and soil texture. Soil conditions, therefore, differed among the main plots on which each CRP was grown. In the season 2019/20, the main plots, on which W1 and W3 were grown, varied the most with more favourable conditions for W3. The soil of all main plots was classified according to the German Soil Classification System (Wittmann *et al.* 1997) in each plot, but at least in the middle of four related plots up to a depth of 100 cm. The soil for the main plot, where W3 was grown in 2019/20, was mainly classified as a Cumulic Anthrosol with humus content and influenced by groundwater. This soil type has a good water-holding capacity and typically a good CEC and high phosphorus (P_2O_5) content (Driessen 2001). In contrast, the main plot, on which W1 was grown in 2019/20 and W3 in 2021/22, was mainly classified as a Stagnosol with partially carbonate in the subsoil. Characteristic for Stagnosols is a change of swelling and reduction, which causes drought and the migration of nutrients in deeper soil layers.

Green area index, intercepted radiation and radiation use efficiency

The measurement of the Green Area Index (GAI) was conducted biweekly during the main growing season from the beginning of April until the end of July with spectral data taken with the Parrot Sequoia camera (Parrot Drones SAS, Paris, France) as described in Bukowiecki et al. 2019. As the development of the GAI on a daily basis is important for further information such as the amount of intercepted radiation, the GAI of each sampling date was interpolated linearly between the date of plant emergence (10 days after sowing, GAI set to 0.03) and the first sampling date and between the last sampling date and the date of harvest (GAI set to 0). Between the sampling dates, a locally weighted scatterplot smoothing (LOESS) was applied by using the loess function in base R (R Core Team 2022), as described in Rose and Kage 2019. The smoothing parameter α was set to 0.65 in 2019/20, to 0.6 in 2020/21 and to 0.5 in 2021/22.

The interpolated GAI curves were then used to calculate Q on a daily basis by Eq. (2) according to Lambert–Beers law (Monsi and Saeki 1953):

$$Q = PAR \times \left(1 - exp^{-k \times GAI}\right) \qquad (2)$$

where PAR is the photosynthetically active radiation estimated as 50% of the global radiation measured by a nearby weather station. The extinction coefficient k was set to 0.7 (Ratjen and Kage 2018; Rose and Kage 2019), and the GAI was extracted from the growth curves for each day. The calculated daily values of Q were used to cumulate the amount of Q during the time periods from plant emergence to anthesis (BBCH 59) (Meier 2018) and from anthesis to harvest as well as the total amount of Q during the whole growing season (plant emergence to harvest) for all genotypes and all N rates.

The cumulated intercepted radiation from plant emergence to harvest was used to calculate the RUE at harvest as the relation between total aboveground biomass and Q (Monteith 1977).

Yield

All plots of W1 and W3 were harvested by combine. Grain yield was standardized to 86% dry matter based on the moisture content of a grain subsample. The thousand kernel weight (TKW) was derived from a subsample by weighing 500 kernels. Kernels/m^2 were calculated as grain yield divided by TKW (x 100.000). The total aboveground biomass at harvest can be calculated by using the ratio of grain yield (combine harvest) and HI (hand harvest). As hand harvest was not conducted in all variants, and an earlier field trial at the same site indicated no significant impact of CRP or genotype on HI (Rose and Kage 2019), the HI was set to 0.55 in all variants.

To describe the yield response to N fertilization a quadratic and a quadratic plateau (QP) model was fitted for each replication of the CRP x genotype variants in each growing season. Both models were able to describe the yield response with a small root mean square error (RMSE). The QP model showed a significantly smaller RMSE. For this reason, the QP model was chosen.

Table 1. Amount of N fertilizer (kg N/ha) applied at the specific growth stage

	Time of Application			
	Beginning of Growth in Spring	Beginning of Stem Elongation	Ear Emergence	Total Amount
N1	0	0	0	0
N2	40	40	40	120
N3	80	80	80	240
N4	120	120	120	360

The economic optimal amount of N fertilizer (N_{opt}) was calculated with the product price for bread wheat (250 €/Mg) and the price for N fertilizer (1.5 €/kg) as a mean of the three years of this study (from 2020 to 2022). N_{opt} is the amount of N fertilizer where the returns of the product price are maximized over the costs for N fertilizer (Bachmaier and Gandorfer 2012). The yield that would be achieved with N_{opt} is the optimum yield (Y_{opt}).

Statistical analysis

All data processing was done using the statistical environment R 4.2.1 (R Core Team 2022). Data visualization was done using the package *ggplot2* (Wickham 2016) and *sjplot* (Lüdecke 2023). Linear mixed effects models (Eq. (3)) were defined by using the package *lme4* (Bates *et al.* 2015). All statistical tests were performed with a significance level of $P = 0.05$. Analysis of variances (ANOVAs) were performed by using the package *car* (Fox and Weisberg 2019), followed by multiple contrast tests with the package *lsmeans* (Lenth 2016).

Due to the experimental design, the year effect could not clearly be separated from the effect of CRP. W1 in 2019/20 and W3 in 2021/22 were grown on the same main plot. No other main plot was used twice for W1 and W3 in the three growing seasons of this study. The linear mixed effects model can calculate the impact of the main plot as a random effect because of the main plot that was used for both CRP. The year effect could not be calculated due to the experimental design, as it was included as random factor in the linear mixed effects model.

The linear mixed effects model (Eq. (3)) includes the fixed factors as well as their interaction terms (two-fold and three-fold). In case of no significance interaction terms were left out in further analysis. Appropriate random effects for the experimental design were also considered:

$$Y = (CRP + N\ level + Genotype)^3 + (1|\ main\ plot/replication) + (1|\ year) \quad (3)$$

where Y is Q pre-anthesis, Q post-anthesis, Q and RUE, kernels/m^2, TKW and grain yield.

The impact of Q pre- and post-anthesis on yield and yield components was analysed with Eq. (4)

$$Y = (Q\ pre\ anthesis + Q\ post\ anthesis)^2 + CRP + Genotype + (1|main\ plot/replication) + (1|year) \quad (4)$$

Where Y is kernels/m^2, TKW and grain yield.

Results

Green area index, intercepted radiation and radiation use efficiency

The GAI was shaped primarily by the amount of N fertilizer, with the higher N rates attaining higher GAI values (Fig. 2). In 2020/21 and 2021/22, all genotypes in W1 realized higher GAI values at all N rates throughout the whole season. In 2019/20 the genotypes in W3 developed higher GAI values in N3 and N4 compared to W1. In this year, the canopies of the W3 variants showed a faster development at the beginning of the growing season which resulted in higher maximum GAI values. In all three years, the canopies of W3 in all genotypes and at all N rates showed a faster senescence than the canopies in W1, with the clearest difference in 2021/22.

In line with the GAI curves, the cumulated intercepted radiation (Q) at harvest was higher in W1 in 2020/21 and 2021/2022. In 2019/20, the W3 canopies intercepted more radiation. CRP ($P < 0.001$) and N ($P < 0.001$) fertilization had a significant impact on Q as well as the genotype ($P < 0.001$) (Table 2) with 'Elixer' intercepting the highest amount of PAR in total (Fig. 3) with 378.3 MJ/m^2 in the unfertilized W1 variant and 742.4 MJ/m^2 in the W1 variant with 240 kg N/ha compared to 'Nordkap' (0 kg N/ha: 310.3 MJ/m^2; 240 kg N/ha: 722 MJ/m^2) and 'Tobak' (0 kg N/ha: 309.1 MJ/m^2; 240 kg N/ha: 720.1 MJ/m^2). 'Elixer' showed the highest decrease in Q total in the unfertilized variant, intercepting 111.2 MJ/m^2 less than in W1, whereas 'Tobak' had the smallest difference in the high fertilized variants with 40.9 MJ/m^2 less in W3 over all genotypes and all N rates.

Q pre- and post-anthesis were both significantly affected by CRP (Q pre-anthesis: $P < 0.001$, Q post-anthesis: $P < 0.05$), N rate (Q pre-anthesis: $P < 0.001$, Q post-anthesis: $P < 0.001$) and genotype (Q pre-anthesis: $P < 0.001$, Q post-anthesis: $P < 0.001$). In addition, Q post-anthesis is the only yield parameter which is significantly affected by the interaction of CRP x genotype (<0.05) (Table 2). In 2019/20, the W3 canopies intercepted more radiation pre-anthesis, contrasting to the other two growing seasons, where W1 intercepted more PAR pre-anthesis. The intercepted radiation post-anthesis was higher in W1 in all three years. 'Elixer' intercepted the highest amount of PAR pre- and post-anthesis (Fig. 3), with a higher difference to 'Nordkap' and 'Tobak' post-anthesis at low N rates (Fig. 4 & Fig. 5). 'Tobak' intercepted the highest amount of radiation in W3 post-anthesis and showed the lowest decrease compared to W1 ('Tobak': −12.5 MJ/m^2 - −28.4 MJ/m^2; 'Elixer': −23.3 MJ/m^2 - −48.8 MJ/m^2; 'Nordkap': −22.1 MJ/m^2 - −34.2 MJ/m^2).

The RUE at harvest for all genotypes in all N rates was significantly lower in W3 ($P < 0.01$) (Fig. 3). The genotype ($P < 0.001$) had a significant impact on the RUE (Table 2). But compared to Q, where 'Elixer' intercepted the highest amount of PAR, 'Tobak' showed a higher RUE (Fig. 3) and was also the only genotype that had the same RUE in W1 and W3 in the fertilized variants.

Yield

Grain yield was significantly affected by CRP ($P < 0.05$), as it declined in W3 (4.1 Mg/ha – 10.2 Mg/ha; W1: 2.5 Mg/ha – 9.5 Mg/ha) in all four N rates as well as in all three growing seasons, even in 2019/20 when W3 was grown on more favourable site conditions. N fertilization ($P < 0.001$) increased the yield significantly with increasing N rates in W1 and W3 in all years (Fig. 6; Fig. 7). The genotype did not have a significant impact on yield (Table 2). N_{opt} and Y_{opt} were not significantly affected by CRP or genotype (Table 2; Table 3).

Table 2. ANOVA results for main effects and interactions according to Eq. (3)

	CRP	N	G	CRPxN	CRPxG	NxG
Q pre-anthesis	<0.001	<0.001	<0.001	<0.05	n.s.	n.s.
Q post-anthesis	<0.05	<0.001	<0.001	n.s.	<0.05	n.s.
Q total	<0.001	<0.001	<0.001	n.s.	n.s.	n.s.
RUE	<0.01	<0.001	<0.001	<0.05	n.s.	n.s.
Kernels/m^2	<0.05	<0.001	0.001	<0.05	n.s.	n.s.
TKW	<0.05	<0.001	<0.001	<0.01	n.s.	n.s.
Grain Yield	<0.05	<0.001	n.s.	n.s.	n.s.	n.s.

CRP, crop rotational position; N, nitrogen rate; G, genotype; Q, radiation intercepted by the canopy; RUE, radiation use efficiency, TKW, thousand kernel weight.
Effects are considered as not significant (n.s.) at $P \geq 0.05$.

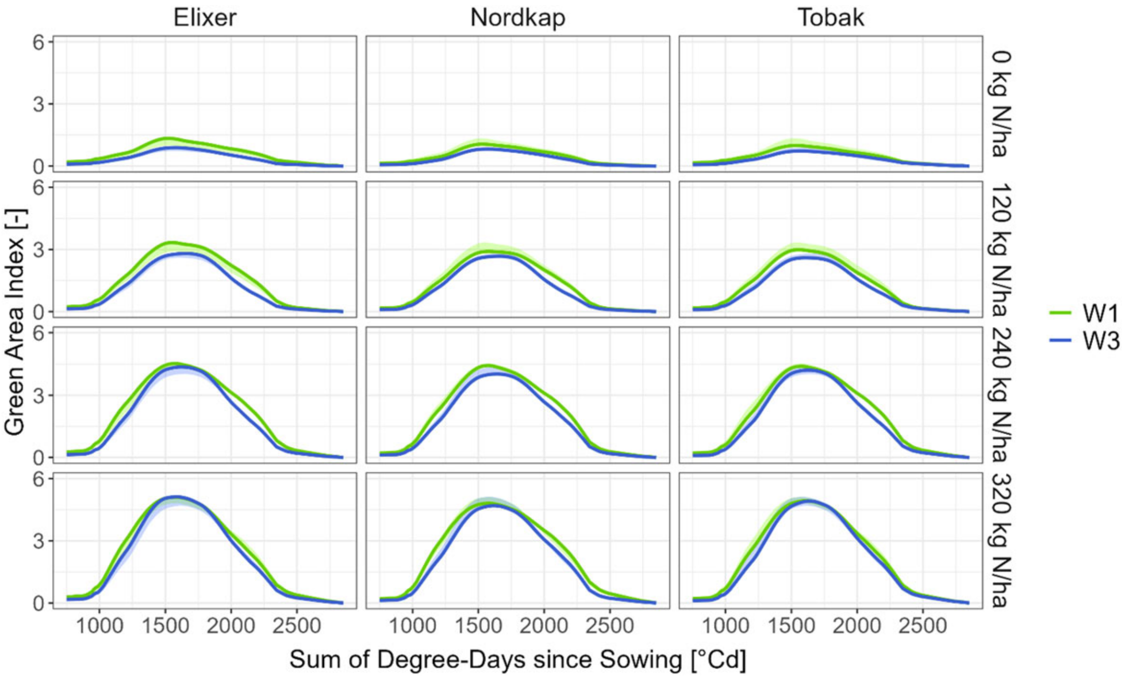

Figure 2. Green Area Index courses for both crop rotational positions (CRP) of the three genotypes in all nitrogen (N) rates. Lines represent the mean over all three growing seasons for each genotype in both CRP in each N rate. Ribbons represent the mean over all growing seasons and all genotypes for each CRP in each N rate. Sum of degree days since sowing were calculated with a base temperature of 0 °C.

In contrast to the grain yield, kernels/m^2 and TKW were significantly affected by the genotype (kernels/m^2: $P < 0.001$, TKW: $P < 0.001$) (Table 2). ‘Nordkap’ achieved the lowest number of kernels/m^2 (W1: 7671 kernels/m^2 – 19644 kernels/m^2; W3: 5567 kernels/m^2 – 17809 kernels/m^2) and the highest TKW (W1: 48.4 g – 52.9 g; W3: 45.5 g – 50.9 g) in both CRP and at all N rates. ‘Elixer’ on the other hand had the highest number of kernels/m^2 (W1: 9010 kernels/m^2 – 21331 kernels/m^2; W3: 6065 kernels/m^2 – 19942 kernels/m^2) and the lowest TKW (W1: 45.6 g – 49 g; W3: 42 g – 50.9 g). ‘Tobak’ had the highest TKW in 2021/22, but the kernels/m^2 were not affected. The TKW increased most with moderate N fertilization whereas more kernels/m^2 were formed with higher N fertilization (Fig. 6). The grain yield (Q pre-anthesis: $P < 0.001$, Q post-anthesis: $P < 0.01$) as well as the yield components kernels/m^2 (Q pre-anthesis: $P < 0.001$, Q post-anthesis: $P < 0.05$) and TKW (Q pre-anthesis: $P < 0.001$, Q post-anthesis: $P < 0.001$) were significantly affected by Q pre- and post-anthesis as well as by their interaction. The CRP had no significant impact on the relation between the intercepted radiation and the yield components (Table 4).

Discussion

The aim of this study was to analyse effects of CRP in interaction with the genotype and different rates of N fertilizer on yield formation of winter wheat in a high-yielding environment. Therefore, besides grain yield itself, effects on yield components and the terms of the Monteith yield equation were analysed. The CRP had significant effects on Q and RUE of wheat which contributed to the reduction of yield and yield components in W3. The three genotypes had different responses to the CRP in the intercepted radiation post-anthesis, which resulted in different N response curves in W3. The experimental design, however, limited

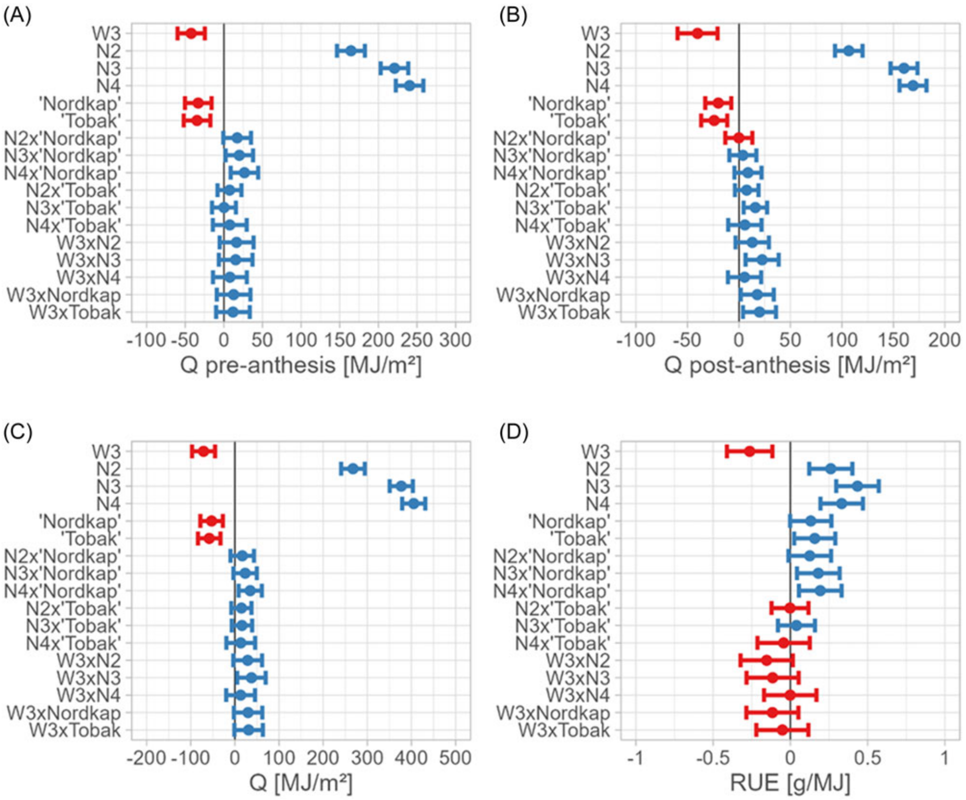

Figure 3. Effect size (dots = mean difference) with 95 %-confidence intervals from the linear mixed effects model of crop rotational position, nitrogen (N) rate and genotype as well as their interaction on selected values of radiation interception (A: radiation intercepted by the canopy (Q) pre-anthesis (MJ/m^2), B: Q post-anthesis (MJ/m^2), C: Q total (MJ/m^2), D: radiation use efficiency (g/MJ). The intercept is the unfertilized W1 (first year of wheat following oilseed rape) variant of the genotype 'Elixer' (A: 231.3 MJ/m^2, B: 145 MJ/m^2, C: 363.9 MJ/m^2, D: 2 g/MJ).

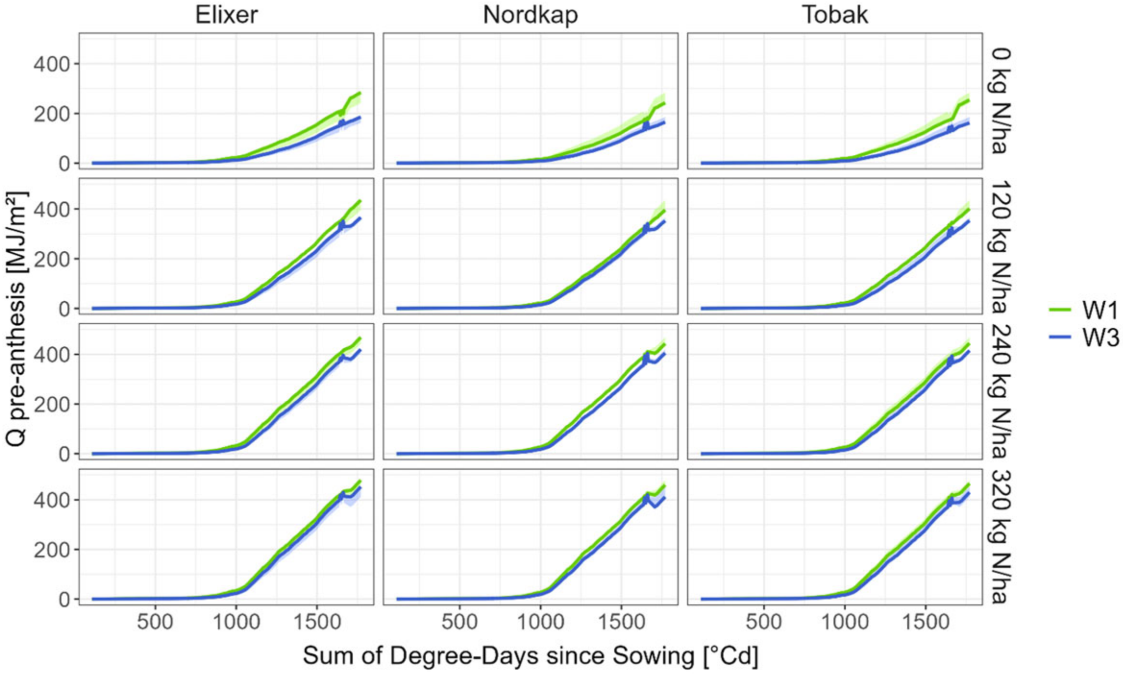

Figure 4. Intercepted radiation pre-anthesis for both crop rotational positions (CRP) of the three genotypes in all nitrogen (N) rates. Lines represent the mean over all three growing seasons for each genotype in both CRP in each N rate. Ribbons represent the mean over all growing seasons and all genotypes for each CRP in each N rate. Sum of degree days since sowing were calculated with a base temperature of 0 °C.

to some extend the analysis, as the interaction year specific effects with the other treatment effects could not be resolved.

The yield reduction in W3 is in accordance with the fact that wheat yield declines in a beginning monoculture and was also observed by others (Christen 1998; Kirkegaard *et al.* 1994; Sieling *et al.* 2005; Sieling *et al.* 2007). An unfavourable CRP, in terms of grain yield, cannot be compensated by a higher amount of N fertilization (Angus *et al.* 1991; Christen *et al.* 1992). However,

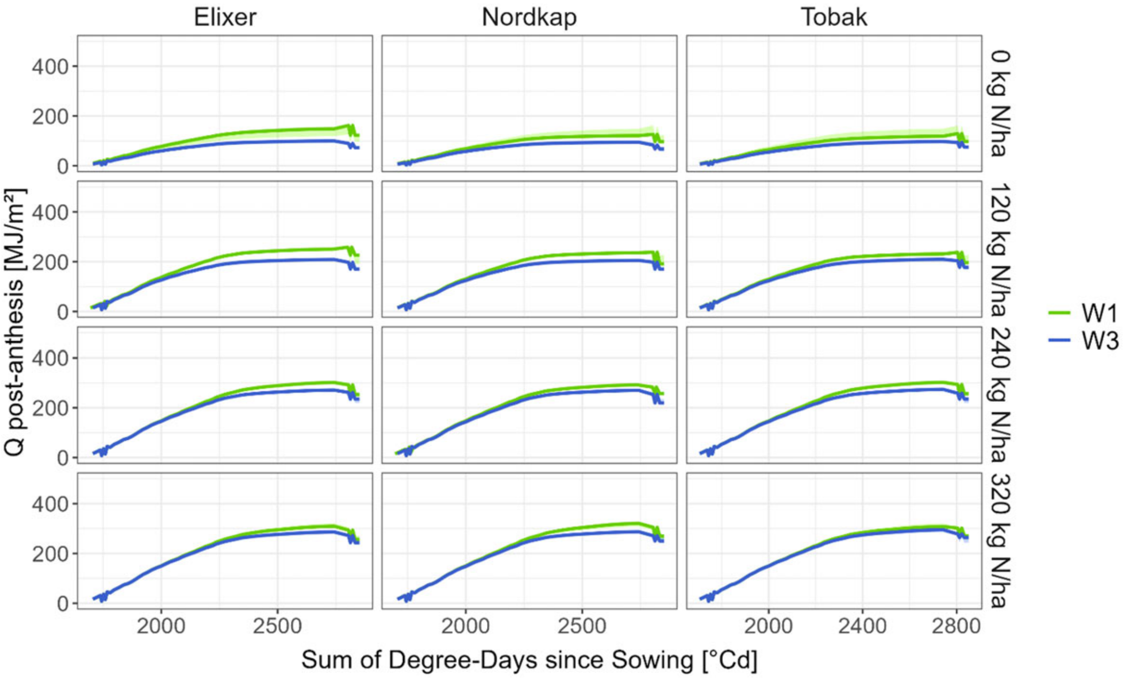

Figure 5. Intercepted radiation post-anthesis for both crop rotational positions (CRP) of the three genotypes in all nitrogen (N) rates. Lines represent the mean over all three growing seasons for each genotype in both CRP in each N rate. Ribbons represent the mean over all growing seasons and all genotypes for each CRP in each N rate. Sum of degree days since sowing were calculated with a base temperature of 0 °C.

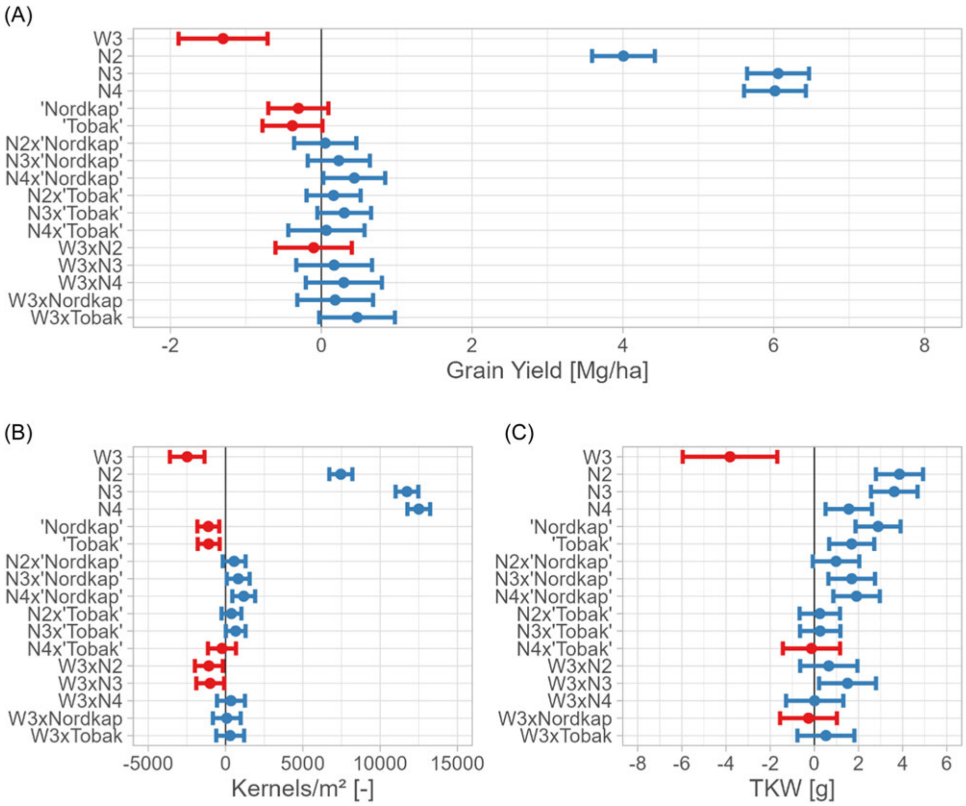

Figure 6. Effect size (dots = mean difference) with 95 %-confidence intervals from the linear mixed effects model of crop rotational position, nitrogen (N) rate and genotype as well as their interaction on selected yield parameters (A: Grain yield (Mg/ha), B: Kernels/m^2 (-), C: Thousand kernel weight (g). The intercept is the unfertilized W1 (first year of wheat following oilseed rape) variant of the genotype 'Elixer' (A: 4.1 Mg/ha, B: 45. 8 g, C: 8910.8 Kernels/m^2).

Kirkegaard *et al.* 1997 reported that the yield decline could be overcome with higher N fertilization.

The yield decline in W3 occurred at all N rates and was composed by a reduction in the yield parameters kernels/m^2 and TKW at all N rates and all genotypes. Here, the year effect was also obvious, but could not further be analysed. It was reported that earlier senescence post-anthesis resulted in higher N remobilization from the vegetative plant parts to the grain (Gaju *et al.* 2016),

Table 3. Economic optimal nitrogen fertilization rate (N_{opt}) (kg N/ha) and grain yield at economic optimal fertilization rate (Y_{opt}) (Mg/ha) of the three genotypes with different crop rotational positions (CRP)

CRP	Genotype	N_{opt}	Y_{opt}
W1	*Elixer*	239.1	9.8
W1	*Nordkap*	269.9	9.9
W1	*Tobak*	249.5	10
W3	*Elixer*	273	9.1
W3	*Nordkap*	262.8	8.8
W3	*Tobak*	280	9.4

W1, first year of wheat following oilseed rape; W3, third year of wheat following oilseed rape.

but also to lower grain yields itself (Waters *et al.* 2009). In wheat grown after wheat, higher N concentration in the grain could be observed (Sieling *et al.* 2005), which was also the case in the data of this study (data not shown).

The economic optimally amount of N fertilization was higher in W3 but led to lower yields compared to W1. Therefore, an unfavourable CRP should be avoided from an environmental as well as from an economic point of view.

A significant interaction between genotype and *Ggt*-infection is dependent on year (van Toor *et al.* 2016). There are also indications for such an interaction in the data of this study, but it is not possible to statistically proof this due to the experimental design. 'Elixer' tended to achieve higher yields at lower N rates. This resulted in a higher intercept for 'Elixer' compared to the other two genotypes in the response curves in W1. In contrast, the three genotypes had the same intercept in the N response curves in W3, but here the slopes differentiated with increasing N rates with 'Tobak' showing the highest response curve.

The most sensitive time period for yield formation is considered to be the weeks before anthesis and 7 days after anthesis (Slafer *et al.* 2021), where yield formation is source-limited (Reynolds *et al.* 2022). During stem elongation until anthesis, the final number of kernels/m^2 is set (Miralles and Slafer 2007). During this phase floret development and grain abortion takes place, which are most susceptible to environmental stress factors (González *et al.* 2011; Reynolds *et al.* 2012). As a general decline in kernels/m^2 in W3 was observed at all N rates, it can be assumed that the CRP had already an impact on yield formation pre-anthesis. The fact that the impact of environmental stress is higher than gene control during this phase (Garcia *et al.* 2011) is supported by 'Elixer' developing the highest number of kernels/m^2 in general but showing also the highest decline in W3.

The development of the GAI throughout the growing season was primarily shaped by the amount of N fertilization. But an effect of the CRP could also be observed with generally lower GAI values and a faster decline in W3. The faster decline of the GAI curves in W3 compared to W1 can be related to an earlier onset of senescence of the W3 canopies. Earlier senescence of plant material is related to an earlier lack of photosynthetic activeness (Sultana *et al.* 2021). This is a process coordinated by a complex gene network and starts when the plant enters the reproductive phase (Sultana *et al.* 2021). Although senescence is mainly controlled by the developmental stage, it is also a response to environmental stress factors (Lim *et al.* 2007). As these factors include the infection with pathogens, the earlier senescence of the W3 canopies could be related to a higher disease pressure which often occurs in a beginning monoculture (van Toor *et al.* 2016). The differences between the growing seasons in the GAI development of W1 and W3 were obvious, but could not further be interpreted.

Splitting the amount of intercepted radiation in phases pre- and post-anthesis gives a more detailed insight in the influence of CRP to yield formation. The amount of intercepted radiation pre-anthesis is correlated to the formation of kernels/m^2 at harvest (Fischer 1985). This is in accordance with our observation of W3 showing a reduction of Q pre-anthesis as well as a reduction of kernels/m^2. A correlation for genotypes with a longer phase of stem elongation and higher grain yields built by a higher number of kernels/plant was reported by Garcia *et al.* 2011. In this study, significant differences between the genotypes were also observed for Q pre-anthesis and kernels/m^2 with 'Elixer' intercepting the highest amount of PAR pre-anthesis and developing the most kernels/m^2. A general effect on higher yields built by a higher number of kernels/m^2 could not be observed. But Elixer' developed the highest yields at low N rates in W1.

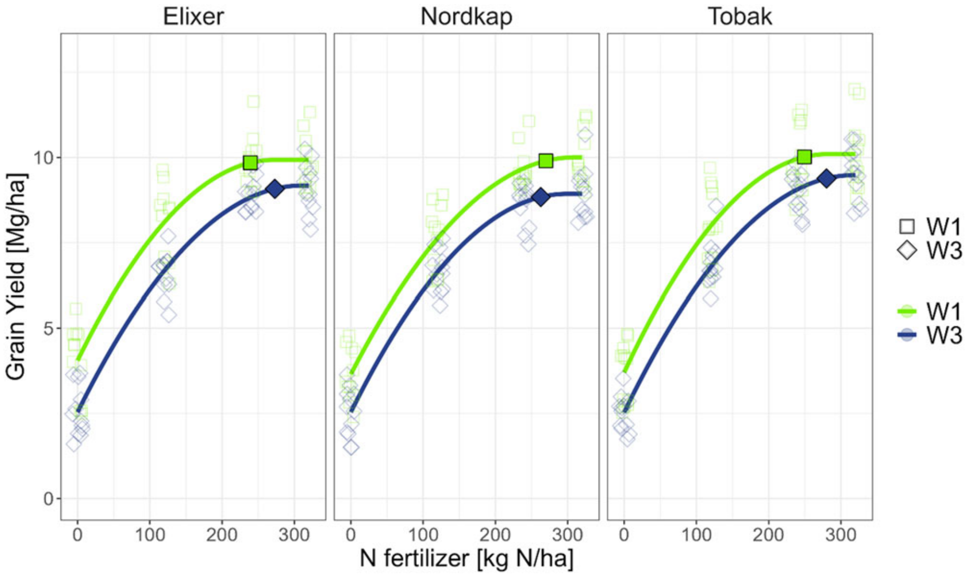

Figure 7. Quadratic-plateau yield functions of the three genotypes in both crop rotational positions (CRP) to nitrogen (N) fertilization. Blank symbols represent the measured grain yield of each plot and full symbols stand for the calculated economic optimum rate of N fertilization of each genotype in both CRP.

Table 4. ANOVA results for main effects and interactions according to Eq. (4)

	Q pre-anthesis	Q post-anthesis	CRP	Genotype	Q pre-anthesis x Q post-anthesis
Kernels/m^2	< 0.001	< 0.05	n.s.	< 0.001	< 0.001
TKW	< 0.001	< 0.001	n.s.	< 0.001	< 0.001
Grain Yield	< 0.001	< 0.01	n.s.	< 0.001	< 0.001

Q, radiation intercepted by the canopy; CRP, crop rotational position; N, nitrogen rate; G, genotype, TKW, thousand kernel weight.
Effects are considered as not significant (n.s.) at $P \geq 0.05$.

As 'Elixer' intercepted the highest amount of PAR pre-anthesis it can be assumed that this genotype established a higher vegetative biomass pre-anthesis. This seemed to be an advantage in yield formation, especially with less N fertilization. But this advantage could not be kept at higher N rates, especially under adverse growing conditions caused by an unfavourable CRP in W3.

After anthesis, the start of N remobilization from the vegetative plant parts to the developing seeds starts and is correlated with its onset of senescence (Sinclair and deWit 1975). During that time, the final TKW is formed and yield formation is mostly sink limited (Reynolds *et al.* 2022). In this study, a general reduction in TKW was observed in W3. This may partly be explained by the earlier decline of GAI in the W3 variants, as a delayed senescence provides a longer period of leave photosynthesis during grain-filling (Thomas and Howarth 2000) which is also connected to a longer period of N uptake that in return can contribute to grain-filling and maintaining the photosynthetic active plant parts (Foulkes *et al.* 2009). On the other hand, Acreche and Slafer 2009 reported a decreasing aboveground biomass post-anthesis if spikes had been trimmed. This shows a response from the plants to a lower number of kernels/m^2. As for this study, the W3 variants had established less kernels/m^2, the earlier decline in GAI might also be a response to a lower sink size during grain filling. The amount of intercepted PAR post-anthesis has also an impact on the formation of kernels/m^2 (Sabir *et al.* 2023), which could in general also be observed for the yield formation in W1 and W3.

A lower number of kernels/m^2 leads also to a lower RUE (Acreche *et al.* 2009; Acreche and Slafer 2011). This is in accordance with the W3 variants showing a reduced RUE. In contrast, 'Elixer' built the highest number of kernels/m^2 between the genotypes but developed the lowest RUE.

Delayed senescence can also be seen as the possibility of canopies to respond to changing environmental conditions (Thomas and Ougham 2014) and it is as well-dependent on the genotype (Cook *et al.* 2021; Rebetzke *et al.* 2016). In this study, 'Elixer' intercepted the highest amount of PAR post-anthesis in W1. But 'Tobak' showed the significant interaction between CRP x genotype for Q post-anthesis, which indicates a better adaptation for this genotype to unfavourable environmental conditions caused by the CRP. As 'Tobak' had also the highest response curve in W3, it seems that the ability to maintain the photosynthetic active plant material post-anthesis longer might be a possibility to partly compensate an unfavourable CRP.

Conclusions

The results of this study showed a decline in yield and yield components for wheat grown in a beginning monoculture. A reduction in kernels/m^2 and kernel mass was observed, which could be interpreted as a first hint of sink limitation. But the analysis of yield formation with the Monteith equation revealed a decrease of intercepted radiation as well as RUE. The reduction was observed early in the season when the final number of kernels/m^2 was set as well as post-anthesis. This leads to the assumption that yield formation for wheat grown in an unfavourable CRP is rather source limited. A significant interaction of CRP x genotype was observed with 'Tobak' intercepting the highest amount of PAR post-anthesis when grown in a beginning monoculture. Combined with a higher response curve compared to the other two genotypes analysed in this study, it might be that this trait will be useful to partly overcome the limitation in yield formation of an unfavourable CRP. This knowledge might be helpful in the breeding process for new varieties to contribute to more stable yields to fulfil the worldwide growing demand for wheat as a staple crop.

Acknowledgements. We thank the team of the Hohenschulen Experimental Farm for their excellent work, Doris Ziermann and Gunda Schnack for their help and support with the field work and Prof. Mario Hasler for statistical advice.

Author contributions. Conceptualization, K.P., H.K.; data curation K.P., N.H.; formal analysis K.P.; writing – original draft, K.P.; writing – review and editing J.B., N.H., H.K.; visualization K.P., J.B.; funding acquisition H.K.; project administration H.K.; supervision H.K.

Funding statement. This work took place in the joint research project 'Rhizosphere Processes and Yield Decline in Wheat Crop Rotations' (RhizoWheat) and was funded by the German Federal Ministry of Education and Research (Funding reference no. 031B0910C).

Competing interests. None.

Ethical standards. Not applicable.

References

Acreche MM, Briceño-Félix G, Martín Sánchez JA and Slafer GA (2009) Radiation interception and use efficiency as affected by breeding in Mediterranean wheat. *Field Crops Research* **110**, 91–97.

Acreche MM and Slafer GA (2009) Grain weight, radiation interception and use efficiency as affected by sink-strength in Mediterranean wheats released from 1940 to 2005. *Field Crops Research* **110**, 98–105.

Acreche MM and Slafer GA (2011) Lodging yield penalties as affected by breeding in Mediterranean wheats. *Field Crops Research* **122**, 40–48.

Angus JF, van Herwaarden AF and How GN (1991) Productivity and break crop effects of winter-growing oilseeds. *Australian Journal of Experimental Agriculture* **31**, 669–677.

Arkebauer TJ, Weiss A, Sinclair TR and Blum A (1994) In defense of radiation use efficiency: a response to Demetriades-Shah et al. (1992). *Agricultural and Forest Meteorology* **68**, 221–227.

Arnhold J, Grunwald D, Braun-Kiewnick A and Koch H-J (2023a) Effect of crop rotational position and nitrogen supply on root development and yield formation of winter wheat. *Frontiers in Plant Science* **14**, 1265994.

Arnhold J, Grunwald D, Kage H and Koch H-J (2023b) No differences in soil structure under winter wheat grown in different crop rotational positions. *Canadian Journal of Soil Science* **103**, 642–649.

Ashraf M and Harris PJ (2013) Photosynthesis under stressful environments: an overview. *Photosynthetica* 193–190.

Asseng S, Kassie BT, Labra MH, Amador C and Calderini DF (2017) Simulating the impact of source-sink manipulations in wheat. *Field Crops Research* **202**, 47–56.

Bachmaier M and Gandorfer M (2012) Estimating uncertainty of economically optimum N fertilizer rates. *International Journal of Agronomy* **2012**, 1–10.

Bates D, Mächler M, Bolker B and Walker S (2015) Fitting linear mixed-effects models using lme4. *Journal of Statistical Software* **67**, 1–48.

Bennett AJ, Bending GD, Chandler D, Hilton S and Mills P (2012) Meeting the demand for crop production: the challenge of yield decline in crops grown in short rotations. *Biological reviews of the Cambridge Philosophical Society* **87**, 52–71.

Bönecke E, Breitsameter L, Brüggemann N, Chen T-W, Feike T, Kage H, Kersebaum K-C, Piepho H-P and Stützel H (2020) Decoupling of impact factors reveals the response of German winter wheat yields to climatic changes. *Global Change Biology* **26**, 3601–3626.

Brisson N, Gate P, Gouache D, Charmet G, Oury F-X and Huard F (2010) Why are wheat yields stagnating in Europe? A comprehensive data analysis for France. *Field Crops Research* **119**, 201–212.

Bullock DG (1992) Crop rotation. *Critical Reviews in Plant Sciences* **11**, 309–326.

Calderini DF and Slafer GA (1998) Changes in yield and yield stability in wheat during the 20th century.

Christen O (1998) Untersuchungen zur Anbautechnik von Winterweizen nach unterschiedlichen Vorfruchtkombinationen. Schriftenreihe des Instituts für Pflanzenbau und Pflanzenzüchtung der Agrarwissenschaftlichen Fakultät der CAU: Kiel.

Christen O, Sieling K and Hanus H (1992) The effect of different preceding crops on the development, growth and yield of winter wheat. *European Journal of Agronomy* **1**, 21–28.

Cook JP, Acharya RK, Martin JM, Blake NK, Khan IJ, Heo H-Y, Kephart KD, Eckhoff J, Talbert LE and Sherman JD (2021) Genetic analysis of stay-green, yield, and agronomic traits in spring wheat. *Crop Science* **61**, 383–395.

Cook RJ (2003) Take-all of wheat. *Physiological and Molecular Plant Pathology* **62**, 73–86.

Driessen PM, (ed.) (2001) *Lecture notes on the major soils of the world.* Rome: Food and Agriculture Organization of the United Nations.

Fischer RA (1985) Number of kernels in wheat crops and the influence of solar radiation and temperature. *The Journal of Agricultural Science* **105**, 447–461.

Fischer RA (2011) Wheat physiology: a review of recent developments. *Crop and Pasture Science* **62**, 95.

Fischer RA (2020) Advances in the potential yield of grain crops. In *Population, Agriculture, and Biodiversity: Problems and Prospects.* University of Missouri Press.

Fischer T, Byerlee D and Edmeades G (2014) *Crop yields and global food security: Will yield increase continue to feed the world?* ACIAR: Canberra.

Foulkes MJ, Hawkesford MJ, Barraclough PB, Holdsworth MJ, Kerr S, Kightley S and Shewry PR (2009) Identifying traits to improve the nitrogen economy of wheat: Recent advances and future prospects. *Field Crops Research* **114**, 329–342.

Fox J and Weisberg S (2019) *An R Companion to Applied Regression.* Thousand Oaks, CA: Sage.

Gaju O, DeSilva J, Carvalho P, Hawkesford MJ, Griffiths S, Greenland A and Foulkes MJ (2016) Leaf photosynthesis and associations with grain yield, biomass and nitrogen-use efficiency in landraces, synthetic-derived lines and cultivars in wheat. *Field Crops Research* **193**, 1–15.

Garcia GA, Serrago RA, Appendino ML, Lombardo LA, Vanzetti LS, Helguera M and Miralles DJ (2011) Variability of duration of pre-anthesis phases as a strategy for increasing wheat grain yield. *Field Crops Research* **124**, 408–416.

Gholizadeh Vazvani M, Dashti H, Saberi Riseh R and Loit E (2025) Association analysis of response to take-all disease with agronomic traits and molecular markers and selection ideal genotypes in bread wheat (Triticum aestivum L.) genotypes. *Molecular Breeding : New Strategies in Plant Improvement* **45**, 36.

González FG, Miralles DJ and Slafer GA (2011) Wheat floret survival as related to pre-anthesis spike growth. *Journal of Experimental Botany* **62**, 4889–4901.

Gutteridge RJ, Bateman GL and Todd AD (2003) Variation in the effects of take-all disease on grain yield and quality of winter cereals in field experiments. *Pest Management Science* **59**, 215–224.

Jamieson PD, Martin RJ, Francis GS and Wilson DR (1995) Drought effects on biomass production and radiation-use efficiency in barley. *Field Crops Research* **43**, 77–86.

Kirkegaard J, Christen O, Krupinsky J and Layzell D (2008) Break crop benefits in temperate wheat production. *Field Crops Research* **107**, 185–195.

Kirkegaard JA, Gardner PA, Angus JF and Koetz E (1994) Effect of Brassica Break Crops on the Growth and Yield of Wheat. *Australian Journal of Agriultural Research* **45**, 529–545.

Kirkegaard JA, Hocking PJ, Angus JF, Howe GN and Gardner PA (1997) Comparison of canola, Indian mustard and Linola in two contrasting environments. II. Break-crop and nitrogen effects on subsequent wheat crops. *Field Crops Research* **52**, 179–191.

Lenth RV (2016) Least-squares means: the R package lsmeans. *Journal of Statistical Software* **69**, 1–33.

Lim PO, Kim HJ and Nam HG (2007) Leaf senescence. *Annual Review of Plant Biology* **58**, 115–136.

Lo Valvo PJ, Miralles DJ and Serrago RA (2018) Genetic progress in Argentine bread wheat varieties released between 1918 and 2011: Changes in physiological and numerical yield components. *Field Crops Research* **221**, 314–321.

Long SP, Zhu X-G, Naidu SL and Ort DR (2006) Can improvemenet in photosynthtesis increase crop yields? *Plant, Cell and Environment* 315–330.

Lüdecke D (2023) sjPlot: Data Visualization for Statistics in Social Science. R package version 2.8.15.

Meier U (2018) Growth stages of mono- and dicotyledonous plants: BBCH Monograph. Open Agrar Repositorium.

Miralles DJ and Slafer GA (2007) Sink limitations to yield in wheat: how could it be reduced? *Journal of Agricultural Science* **145**, 139–149.

Monsi M and Saeki T (1953) Über den Lichtfaktor in den Pflanzengesellschaften und seine Bedeutung für die Stoffproduktion, https://scholar.google.com/scholar?cluster=16183797658627183035&hl=de&as_sdt=0,5#d=gs_cit&t=1721128652370&u=%2Fscholar%3Fq%3Dinfo%3Ay0n_zaajHc0J%3Ascholar.google.com%2F%26output%3Dcite%26scirp%3D1%26scfhb%3D1%26hl%3Dde.

Monteith JL (1977) Climate and the efficiency of crop production in Britain. *Philosophical Transactions of the Royal Society London B* **281**, 277–294.

Moore FC and Lobell DB (2015) The fingerprint of climate trends on European crop yields. *Proceedings of the National Academy of Sciences of the United States of America* **112**, 2670–2675.

O'Connell MG, O'Leary GJ, Whitfield DM and Connor DJ (2004) Interception of photosynthetically active radiation and radiation-use efficiency of wheat, field pea and mustard in a semi-arid environment. *Field Crops Research* **85**, 111–124.

Palma-Guerrero J, Chancellor T, Spong J, Canning G, Hammond J, McMillan VE and Hammond-Kosack KE (2021) Take-All disease: new insights into an important wheat root pathogen. *Trends in Plant Science* **26**, 836–848.

R Core Team (2022) R: A language and environment for statistical computing.: R Foundation for Statistical Computing: Vienna, Austria.

Ratjen AM and Kage H (2018) Predicting the site specific soil N supply under winter wheat in Germany. *Nutrient Cycling in Agroecosystems* **110**, 71–81.

Rebetzke GJ, Jimenez-Berni JA, Bovill WD, Deery DM and James RA (2016) High-throughput phenotyping technologies allow accurate selection of stay-green. *Journal of Experimental Botany* **67**, 4917–4919.

Reynolds M, Foulkes J, Furbank R, Griffiths S, King J, Murchie E, Parry M and Slafer G (2012) Achieving yield gains in wheat. *Plant, Cell & Environment* **35**, 1799–1823.

Reynolds MP, Slafer GA, Foulkes JM, Griffiths S, Murchie EH, Carmo-Silva E, Asseng S, Chapman SC, Sawkins M, Gwyn J and Flavell RB (2022) A wiring diagram to integrate physiological traits of wheat yield potential. *Nature Food* **3**, 318–324.

Rivera-Amado C, Trujillo-Negrellos E, Molero G, Reynolds MP, Sylvester-Bradley R and Foulkes MJ (2019) Optimizing dry-matter partitioning for increased spike growth, grain number and harvest index in spring wheat. *Field Crops Research* **240**, 154–167.

Rose T and Kage H (2019) The Contribution of Functional Traits to the Breeding Progress of Central-European Winter Wheat Under Differing Crop Management Intensities.

Sabir K, Rose T, Wittkop B, Stahl A, Snowdon RJ, Ballvora A, Friedt W, Kage H, Léon J, Ordon F, Stützel H, Zetzsche H and Chen Tsu-Wei (2023) Stage-specific genotype-by-environment interactions determine yield components in wheat. *Nature Plants* **9**, 1688–1696.

Schierenbeck M, Fleitas MC, Miralles DJ and Simón MR (2016) Does radiation interception or radiation use efficiency limit the growth of wheat inoculated with tan spot or leaf rust? *Field Crops Research* **199**, 65–76.

Schnyder H (1993) The role of carbohydrate storage and redistribution in the source-sink relations of wheat and barley during grain filling — a review. *New Phytologist* **123**, 233–245.

Sharma A, Kumar V, Shahzad B, Ramakrishnan M, Singh Sidhu GP, Bali AS, Handa N, Kapoor D, Yadav P, Khanna K, Bakshi P, Rehman A, Kohli SK, Khan EA, Parihar RD, Yuan H, Thukral AK, Bhardwaj R and Zheng B (2020) Photosynthetic response of plants under different abiotic stresses: a review. *Journal of Plant Growth Regulation* **39**, 509–531.

Sieling K, Stahl C, Winkelmann C and Christen O (2005) Growth and yield of winter wheat in the first 3 years of a monoculture under varying N fertilization in NW Germany. *European Journal of Agronomy* **22**, 71–84.

Sieling K, Ubben K and Christen O (2007) Effects of preceding crop, sowing date, N fertilization and fluquinconazole seed treatment on wheat growth, grain yield and take-all. *Journal of Plant Diseases and Protection* **114**, 213–220.

Sinclair TR and deWit CT (1975) Photosynthate and nitrogen requirements for seed production by various crops. *Science* **189**, 565–567.

Slafer GA, Savin R, Pinochet D and Calderini D (2021) *Crop Physiology Case Histories for Major Crops*. Academic Press.

Sultana N, Islam S, Juhasz A and Ma W (2021) Wheat leaf senescence and its regulatory gene network. *The Crop Journal* **9**, 703–717.

Thomas H and Howarth CJ (2000) Five ways to stay green. *Journal of Experimental Botany* **51**, 329–337.

Thomas H and Ougham H (2014) The stay-green trait. *Journal of Experimental Botany* **65**, 3889–3900.

van Toor RF, Chng S, Warren RM, Butler RC, Cromey MG, Craigie RA and McCloy BL (2016) Wheat cultivar susceptibility to Gaeumannomyces graminis var. tritici and influence on Pseudomonas fluorescence numbers in the rhizosphere. *Australasian Plant Pathology* **45**, 595–607.

Voss-Fels KP, Stahl A, Wittkop B, Lichthardt C, Nagler S, Rose T, Chen T-W, Zetzsche H, Seddig S, Majid Baig M, Ballvora A, Frisch M, Ross E, Hayes BJ, Hayden MJ, Ordon F, Leon J, Kage H, Friedt W, Stützel H and Snowdon RJ (2019) Breeding improves wheat productivity under contrasting agrochemical input levels. *Nature Plants* **5**, 706–714.

Waters BM, Uauy C, Dubcovsky J and Grusak MA (2009) Wheat (Triticum aestivum) NAM proteins regulate the translocation of iron, zinc and nitrogen compounds from vegetative tissues to grain. *Journal of Experimental Botany* **60**, 4263–4274.

Wickham H (2016) *Ggplot2: Elegant Graphics for Data Analysis*. Cham: Springer International Publishing; Imprint; Springer.

Wilson DR and Jamieson PD (1985) Models of growth and water use of wheat in New Zealand. In Day W and Atkin RK (eds.). *Wheat Growth and Modelling*. Boston, MA: Springer US; Imprint; Springer, pp. 211–216.

Wittmann O, Blume H-P, Filipinski M and Witt S (1997) Soil Classification of the Federal Republic of Germany. Mitteilung der deutschen Bodenkundlichen Gesellschaft, 253–275.

Appendix

Absolute values as a mean over the three growing seasons for intercepted radiation, yield and yield components

CRP	Genotype	N rate	Q pre-anthesis [MJ/m^2]	Q post-anthesis [MJ/m^2]	Q total [MJ/m^2]	RUE [g/MJ]	Kernels/m^2	TKW [g]	Grain Yield [Mg/ha]
W1	Elixer	0 kg N/ha	234.6	148.9	378.3	2	9010	45.6	4.1
W1	Elixer	120 kg N/ha	393.5	250.4	641.8	2.3	16444	49.6	8.1
W1	Elixer	240 kg N/ha	450	301.9	742.4	2.5	20558	49	10.1
W1	Elixer	320 kg N/ha	466.8	309.6	767	2.4	21331	47	10.2
W1	Nordkap	0 kg N/ha	193.6	121.4	310.3	2.2	7671	48.4	3.7
W1	Nordkap	120 kg N/ha	365.6	235.9	593.1	2.4	14934	51.9	7.7
W1	Nordkap	240 kg N/ha	436.8	292.4	722.3	2.5	18423	52.9	9.7
W1	Nordkap	320 kg N/ha	456.1	321.3	768	2.4	19644	51.4	10.1
W1	Tobak	0 kg N/ha	194.5	119.1	309.1	2.2	7890	47.1	3.7
W1	Tobak	120 kg N/ha	370.7	231.2	593.5	2.4	15646	51.2	8
W1	Tobak	240 kg N/ha	426.8	302.6	720.1	2.5	19815	50.4	10
W1	Tobak	320 kg N/ha	448.2	308.1	746.8	2.5	20435	49.5	10.1
W3	Elixer	0 kg N/ha	171.3	100.1	267.1	1.8	6065	42	2.6
W3	Elixer	120 kg N/ha	356.8	208.9	557.3	2.1	14053	46.8	6.6
W3	Elixer	240 kg N/ha	418	271.4	680.1	2.4	18815	47.6	9
W3	Elixer	320 kg N/ha	446.6	286.3	723.4	2.3	19942	45.7	9.1
W3	Nordkap	0 kg N/ha	153.2	95.1	244.3	1.9	5567	45.3	2.5
W3	Nordkap	120 kg N/ha	342.9	205.2	539.9	2.3	13335	50.2	6.7
W3	Nordkap	240 kg N/ha	403.6	270.3	664.9	2.4	16960	50.9	8.6
W3	Nordkap	320 kg N/ha	428.9	287.1	706.6	2.3	17809	50.3	9
W3	Tobak	0 kg N/ha	142.2	97.8	236.3	2	5662	44.2	2.5
W3	Tobak	120 kg N/ha	328	209.7	529.7	2.4	14010	48.8	6.9
W3	Tobak	240 kg N/ha	397	274.2	662	2.5	18203	49.3	9
W3	Tobak	320 kg N/ha	419.7	295.6	705.9	2.5	19916	47.9	9.5

CRP, crop rotational position; N, nitrogen rate; Q, radiation intercepted by the canopy; RUE, radiation use efficiency; TKW, thousand kernel weight.